

UCSF

UC San Francisco Previously Published Works

Title

Transcriptional activation of RagD GTPase controls mTORC1 and promotes cancer growth

Permalink

<https://escholarship.org/uc/item/76z9v0ff>

Journal

Science, 356(6343)

ISSN

0036-8075

Authors

Di Malta, Chiara
Siciliano, Diletta
Calcagni, Alessia
et al.

Publication Date

2017-06-16

DOI

10.1126/science.aag2553

Peer reviewed



Published in final edited form as:

Science. 2017 June 16; 356(6343): 1188–1192. doi:10.1126/science.aag2553.

TRANSCRIPTIONAL ACTIVATION OF RAGD GTPASE CONTROLS mTORC1 AND PROMOTES CANCER GROWTH

Chiara Di Malta¹, Diletta Siciliano¹, Alessia Calcagni¹, Jlenia Monfregola¹, Simona Punzi², Nunzia Pastore^{1,3}, Andrea N. Eastes⁴, Oliver Davis⁵, Rossella de Cegli¹, Angela Zampelli¹, Luca G. Di Giovannantonio¹, Edoardo Nusco¹, Nick Platt⁶, Alessandro Guida², Margret Helga Ogmundsdottir⁷, Luisa Lanfrancone², Rushika M. Perera⁴, Roberto Zoncu⁵, Pier Giuseppe Pelicci^{2,8}, Carmine Settembre^{1,9,10}, and Andrea Ballabio^{1,3,10,11}

¹Telethon Institute of Genetics and Medicine (TIGEM), via Campi Flegrei, 34, 80078 Pozzuoli (Naples), Italy ²Department of Experimental Oncology, European Institute of Oncology, Milan 20139, Italy ³Jan and Dan Duncan Neurological Research Institute, Houston, TX 77030, USA ⁴Department of Anatomy, and Helen Diller Family Comprehensive Cancer Center, University of California San Francisco, San Francisco, CA 94143 ⁵Department of Molecular and Cellular Biology, and Paul F. Glenn Center for Aging Research, University of California Berkeley, Berkeley, CA 94720 ⁶Department of Pharmacology, University of Oxford, Oxford, UK ⁷Department of Biochemistry and Molecular Biology, University of Iceland, Vatnsmyrarvegur 16, Reykjavik 101, Iceland ⁸Department of Oncology, University of Milan, Milan 20139, Italy ⁹Dulbecco Telethon Institute, Via Campi Flegrei, 34, 80078 Pozzuoli (NA), Italy ¹⁰Medical Genetics Unit, Department of Medical and Translational Science, Federico II University, Via Pansini 5, 80131 Naples, Italy ¹¹Department of Molecular and Human Genetics and Neurological Research Institute, Baylor College of Medicine, Houston, Texas 77030, USA

Abstract

The mechanistic Target Of Rapamycin Complex 1 (mTORC1) is recruited to the lysosome by Rag GTPases and regulates anabolic pathways in response to nutrients. Here we find that MiT/TFE transcription factors, master regulators of lysosomal and melanosomal biogenesis and autophagy, control mTORC1 lysosomal recruitment and activity by directly regulating the expression of RagD. In mice this mechanism mediated adaptation to food availability after starvation and physical exercise and played an important role in cancer growth. Up-regulation of MiT/TFE genes in cells and tissues from patients and murine models of renal cell carcinoma, pancreatic ductal adenocarcinoma, and melanoma triggered RagD-mediated mTORC1 induction, resulting in cell hyper-proliferation and cancer growth. Thus, this transcriptional regulatory mechanism enables cellular adaptation to nutrient availability and supports the energy-demanding metabolism of cancer cells.

Correspondence to: Andrea Ballabio: ballabio@tigem.it.

SUPPLEMENTARY MATERIALS

Materials and Methods

Figs. S1 to S10

Tables S1 to S2

A major determinant of species evolution is the ability to switch between anabolic and catabolic pathways in response to nutrient availability. The nutrient-activated kinase complex mTORC1 promotes biosynthetic processes and inhibits catabolic pathways such as autophagy (1, 2), thus playing a crucial role in the adaptation of the organism to the environment (3, 4). The transcription factors TFEB, TFE3, TFEC and MITF belong to the MiT-TFE family and bind the same target sites in the proximal promoters of overlapping sets of genes (5, 6). TFEB and TFE3 are master transcriptional regulators of lysosomal biogenesis and autophagy (6–8), while MITF regulates melanosomal biogenesis (9). mTORC1 negatively regulates the activity of these transcription factors by phosphorylating critical serine residues, leading to their cytoplasmic retention (8, 10–12). Conversely, during starvation or physical exercise inhibition of mTORC1 and activation of the phosphatase calcineurin leads to TFEB and TFE3 de-phosphorylation and nuclear translocation (13, 14).

We postulated the presence of a feedback loop by which MiT-TFE transcription factors, which are substrates of mTORC1, may in turn influence mTORC1 activity. SiRNA-mediated depletion of either *TFEB* or *TFE3* in HeLa cells significantly decreased mTORC1 activity upon amino-acid administration (Fig. S1A,B). Furthermore, mTORC1 reactivation upon prolonged starvation (15) was inhibited in *TFEB*-silenced cells (Fig. S1C). Overexpression of either wild type or constitutively active *TFEB* and *TFE3* (*TFEB-CA* and *TFE3-CA*) resulted in increased mTORC1 activation upon stimulation with either a complete set of amino acids (Fig. S1A,B; Fig. S2) or solely leucine or arginine, the key amino acids that activate mTORC1 (16) (Fig. 1A,B). Consistently, viral-mediated *TFEB* overexpression in the liver of wild type mice increased mTORC1 signaling (Fig. 1C,D). Conversely, a significant reduction in the rate of protein synthesis and impaired mTORC1 signaling were detected in the livers from *TFEB* liver-specific conditional KO mice (*Tcfef^{lox/lox}; Alb-CRE⁺*; hereafter *Tcfef*-LiKO) (Fig. 1E). In addition, exercised muscle-specific *TFEB* KO mice (*Tcfef^{lox/lox}; Mlc-CRE⁺*; hereafter *Tcfef*-MuKO) showed a reduced induction of mTORC1 activity and protein synthesis in response to leucine after exercise (Fig. 1F). Thus, the effect of a protein meal after exercise on muscle protein synthesis requires TFEB-induced transcriptional activation of mTORC1 signaling.

TFEB overexpression in cells lacking the essential autophagy genes *Atg5* or *Atg7* still resulted in enhanced mTORC1 activity, similar to wild type cells (Fig. S3). Thus, MiT-TFE transcription factors may regulate mTORC1 by a mechanism which is different from autophagy. To identify such a mechanism, we searched for TFEB DNA binding sites, defined as “CLEAR elements” (6), in the promoters of 50 human genes known to play a role in the activation of mTORC1. Among 20 TFEB/TFE3 putative target genes (Table S1,2), the transcript levels of the GTPase *RagD* were the most significantly decreased upon single or combined *TFEB* or *TFE3* silencing (Fig. S4A–C). Conversely, *RagD* was strongly induced in *TFEB*-overexpressing cells both at the mRNA (Fig. 2A; Fig. S4D) and protein levels (Fig. S4E,F). An induction of *RagD* expression was also detected in liver samples from mice injected with Helper Dependent adenovirus (HDAd) containing *TFEB* or *TFE3* (Fig. S4G), while a reduction of *RagD* expression was observed in *TFEB* Li-KO and *TFE3* full KO mice (Fig. S4H). To exert its activity *RagD* and *RagC* need to heterodimerize with *RagA* or *RagB* and to be activated by Folliculin (FLCN), a GTPase activating protein (GAP) (17). *RagC* and FLCN expression levels were also influenced by MiT-TFE genes, albeit to a lesser extent

compared to RagD (Fig 2A; S4A–D). RagD is expressed at very low levels, thus we postulate that RagD is a limiting factor for RagGTPase activity.

Chromatin Immuno-Precipitation (ChiP) and luciferase assay experiments revealed that *RagD* is a direct transcriptional target of TFEB (Fig 2B,C). Thus, we used a CRISPR-Cas9-mediated genome editing approach to delete the most responsive TFEB target site in the *RagD* proximal promoter region in HeLa cells (HeLa-RagD^{promedit}) (Fig 2D). This cell line showed significantly reduced transcript and protein levels of *RagD*, while other mTORC1-related genes were not affected (Fig 2E and S5A), as well as a significant impairment of mTORC1 activation upon amino acid stimulation (Fig 2F and S5B,C). Overexpression of exogenous *RagD* rescued mTORC1 signaling in the HeLa-RagD^{promedit} cell line (Fig S5D). Consistently, viral-mediated *RagD* gene delivery rescued impaired mTORC1 signaling and defective protein synthesis in the livers of *Tcfel*-LiKO mice (Fig 2G). Thus, the transcriptional regulation of *RagD* expression by MiT-TFE transcription factors plays an important role in the control of mTORC1 activity.

TFEB and TFE3 are activated by starvation (7, 18). Consistently, we observed an increase of *RagD* mRNA and protein levels during starvation, which was blunted by silencing of either *TFEB* or *TFE3* (Fig. S6A,B). In addition, we found a significant correlation between starvation-induced TFEB nuclear localization and *RagD* expression levels (Fig S6C,D). Accordingly, fasting and physical exercise in mice induced *RagD* expression in liver and muscle, which was blunted in *TFEB* Li-KO and Mu-KO mice, respectively (S6 E,F). Nutrients induce mTORC1 recruitment to the lysosomal surface via the interaction of Rag GTPases with the Raptor subunit of the mTORC1 complex (19, 20). We detected an increase of amino acid-induced mTORC1 recruitment to the lysosome in *TFEB*-CA overexpressing cells compared with wild type cells (Fig S7A,B), while an opposite effect was observed in *TFEB*-depleted cells as well as in the HeLa-RagD^{promedit} cell line (Fig 3A,B), which was rescued by *RagD* overexpression (Fig 3A). Thus, TFEB-mediated control of RagD promotes the efficient recruitment of mTORC1 to the lysosome.

MiT-TFE are known oncogenes overexpressed in a variety of tumors such as renal cell carcinoma (RCC), melanoma, sarcoma and pancreatic ductal adenocarcinoma (21–23). *TFEB* kidney-specific conditional overexpressing mice display a phenotype that closely recapitulates human RCC (24). We observed hyper-activation of mTORC1 signaling and increased *RagD* transcript levels in both kidney tissues and primary kidney cells from these mice (Fig S8A–C). Treatment with the mTORC1 inhibitor Torin 1 fully rescued the hyper-proliferative phenotype of primary kidney cells (Fig S8D). Similarly, kidney cells derived from a patient with RCC carrying a chromosomal translocation that involves the *TFE3* gene (HCR-59) showed increased *RagD* transcript levels and enhanced mTORC1 signaling (Fig 4A,B). Notably, silencing of either *TFE3* or *RagD* rescued mTORC1 hyper-activation and reduced tumor cell proliferation (Fig S8E,F and 4C). Furthermore, a survey of RNA sequencing data obtained from patients with RCC carrying *TFE3* chromosomal translocations revealed a consistent increase of *RagD* expression levels (Fig S8G) (25). We also analyzed cell lines from patients with Pancreatic Ductal Adenocarcinoma (PDA) in which several *MiT/TFE* genes are up-regulated (23) and found increased *RagD* levels (Fig

S9A,B). Silencing of *TFE3* in two of these cell lines decreased *RagD* levels and rescued mTORC1 hyper-activation (Fig S9C–F).

MITF, another member of the MiT/TFE family, is an established oncogene in melanoma (26). Transient overexpression of *MITF* in HeLa cells induced up-regulation of *RagD* transcript levels and increased mTORC1 activation (Fig S9G,H), indicating that also MITF is able to positively regulate *RagD* expression. Consistently, a cell line from a patient with melanoma, associated with high levels of MITF, 501mel, showed induction of *RagD* expression and increased mTORC1 activation (Fig 4D,E). Notably, silencing of *RagD* was sufficient to significantly revert the hyper-proliferative phenotype of this tumor cell line (Fig 4F). In addition, a survey of published microarray data available for melanoma metastatic patients (TCGA data set) and melanoma cell lines (GEO database) revealed a significant correlation between *MITF* and *RagD* gene expression levels (Fig S9I,J). Importantly, xenotransplantation experiments performed using the 501mel melanoma cell line showed strikingly reduced xenograft tumor growth upon *RagD*-silencing, demonstrating a key role of RagD in promoting tumor growth (Fig 4G,H). In conclusion, we identified an MiT/TFE-RagD-mTORC1-MiT/TFE feedback circuit, whose fine modulation is critical for metabolic adaptation to nutrient availability. Deregulation of this mechanism supports cancer metabolism, thus promoting tumor growth (Fig. S10).

Supplementary Material

Refer to Web version on PubMed Central for supplementary material.

Acknowledgments

We are grateful to Drs. Maria Antonietta De Matteis, Graciana Diez-Roux and Gennaro Napolitano for helpful suggestions. We thank Drs. AnnaChiara Salzano and Emanuela De Gennaro for technical assistance. This work was supported by grants from the Italian Telethon Foundation (TGM11CB6), the European Research Council Advanced Investigator grant no. 250154 (CLEAR) (A.B.) and no 341131 (InMec) (P.G.P.); US National Institutes of Health (R01-NS078072) (A.B.) and the Associazione Italiana per la Ricerca sul Cancro (A.I.R.C.) to A.B (IG 2015 Id 17639) and C.S. (IG 2015 Id 17717).

REFERENCES AND NOTES

1. Rabinowitz JD, White E. *Science*. 2010; 330:1344–1348. [PubMed: 21127245]
2. Saxton RA, Sabatini DM. *Cell*. 2017; 169:361–371.
3. Howell JJ, Manning BD. *Trends Endocrinol Metab TEM*. 2011; 22:94–102. [PubMed: 21269838]
4. Watson K, Baar K. *Semin Cell Dev Biol*. 2014; 36:130–139. [PubMed: 25218794]
5. Steingrimsson E, Copeland NG, Jenkins NA. *Annu Rev Genet*. 2004; 38:365–411. [PubMed: 15568981]
6. Sardiello M, et al. *Science*. 2009; 325:473–477. [PubMed: 19556463]
7. Settembre C, et al. *Science*. 2011; 332:1429–1433. [PubMed: 21617040]
8. Martina JA, et al. *Sci Signal*. 2014; 7:ra9. [PubMed: 24448649]
9. Hodgkinson CA, et al. *Cell*. 1993; 74:395–404. [PubMed: 8343963]
10. Settembre C, et al. *EMBO J*. 2012; 31:1095–1108. [PubMed: 22343943]
11. Rocznik-Ferguson A, et al. *Sci Signal*. 5:ra42. [PubMed: 22692423]
12. Martina JA, Puertollano R. *J Cell Biol*. 2013; 200:475–491. [PubMed: 23401004]
13. Settembre C, Fraldi A, Medina DL, Ballabio A. *Nat Rev Mol Cell Biol*. 2013; 14:283–296. [PubMed: 23609508]

14. Medina DL, et al. *Nat Cell Biol.* 2015; 17:288–299. [PubMed: 25720963]
15. Yu L, et al. *Nature.* 2010; 465:942–946. [PubMed: 20526321]
16. Ban H, et al. *Int J Mol Med.* 2004; 13:537–543. [PubMed: 15010853]
17. Tsun ZY, et al. *Mol Cell.* 2013; 52:495–505. [PubMed: 24095279]
18. Martina JA, et al. *Sci Signal.* 2014; 7:ra9. [PubMed: 24448649]
19. Sancak Y, et al. *Science.* 2008; 320:1496–1501. [PubMed: 18497260]
20. Kim E, Goraksha-Hicks P, Li L, Neufeld TP, Guan KL. *Nat Cell Biol.* 2008; 10:935–945. [PubMed: 18604198]
21. Haq R, Fisher DE. *J Clin Oncol Off J Am Soc Clin Oncol.* 2011; 29:3474–3482.
22. Kauffman EC, et al. *Nat Rev Urol.* 2014; 11:465–475. [PubMed: 25048860]
23. Perera RM, et al. *Nature.* 2015; 524:361–365. [PubMed: 26168401]
24. Calcagni A, et al. *eLife.* 2016; 5doi: 10.7554/eLife.17047
25. Malouf GG, et al. *Clin Cancer Res Off J Am Assoc Cancer Res.* 2014; 20:4129–4140.
26. Tsao H, Chin L, Garraway LA, Fisher DE. *Genes Dev.* 2012; 26:1131–1155. [PubMed: 22661227]
27. Halaban R, Cheng E, Smicun Y, Germino J. *J Exp Med.* 2000; 191:1005–1016. [PubMed: 10727462]
28. Primot A, et al. *Pigment Cell Melanoma Res.* 2010; 23:93–102. [PubMed: 19895547]
29. Steingrimsson E, et al. *Proc Natl Acad Sci U S A.* 2002; 99:4477–4482. [PubMed: 11930005]
30. Settembre C, et al. *Nat Cell Biol.* 2013; 15:647–658. [PubMed: 23604321]
31. Ezaki J, et al. *Autophagy.* 2011; 7:727–736. [PubMed: 21471734]

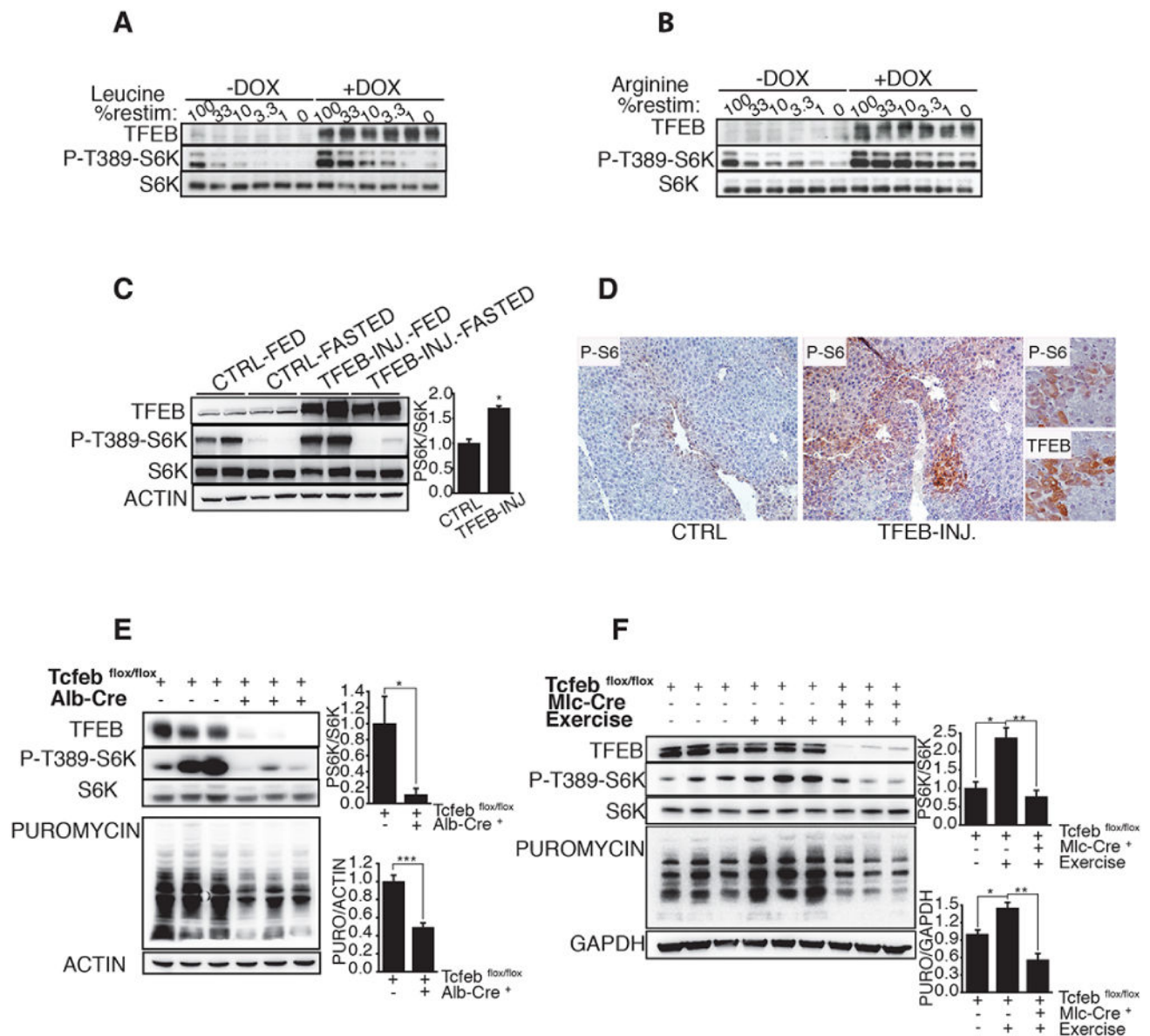


Fig 1. MiT/TFE transcription factors regulate mTORC1 activity both *in vitro* and *in vivo*
 (A,B) Representative immuno-blotting analysis of TFEB, phospho-S6K and S6K in Tet-ON *TFEB-CA* cell line untreated (-DOX) or treated with Doxycycline (+DOX) for 24h. Cells were starved for a.a. for 50 min (0) and stimulated with decreasing levels (expressed as % of concentration in RPMI medium) of leucine (A) or arginine (B) for 20 min. (C) C57BL6 mice injected with a Helper-Dependent adenovirus (HDAd) expressing human *TFEB* under the control of a liver-specific promoter (TFEB-INJ.), or with PBS (CTRL) were starved for 22h (FASTED), and then refeed for 2h (FED). Liver lysates were analyzed for levels of indicated proteins. Actin was used as loading control. The plot shows ratio of phosphorylated S6K/pan-S6K (mean of three independent experiments). (D) Immunohistochemistry analysis of liver sections from mice injected with saline PBS (CTRL) or HDAd-*TFEB* (TFEB-INJ.). Tissues were stained for serine 240/244 phosphorylated-S6 (P-S6). Insets show overlapping P-S6 and TFEB immunostainings in two

consecutive 5 μ m liver sections isolated from HDad-TFEB injected mice. (E) Liver samples from mice with indicated genotypes were analyzed for the levels of S6K phosphorylation and puromycin incorporation. The plots show the ratios of phosphorylated S6K/pan-S6K and puromycin/actin expressed as relative to control mice (Tcfef^{flox/flox}). (F) Phosphorylation of S6K and levels of puromycin incorporation analysis in muscle samples from mice with indicated genotypes after oral gavage of leucine. Mice were exercised where indicated. The plots show ratios of phosphorylated S6K/pan-S6K and puromycin/GAPDH. The plots in (C), (E) represent means of triplicates \pm SEM, Student t-test. The plot in (F) represent means \pm SEM; N=3; Anova (one-way) followed by Tukey's test. In (C), (E), (F) *p < 0.05 **=p < 0.01, ***p < 0.001.

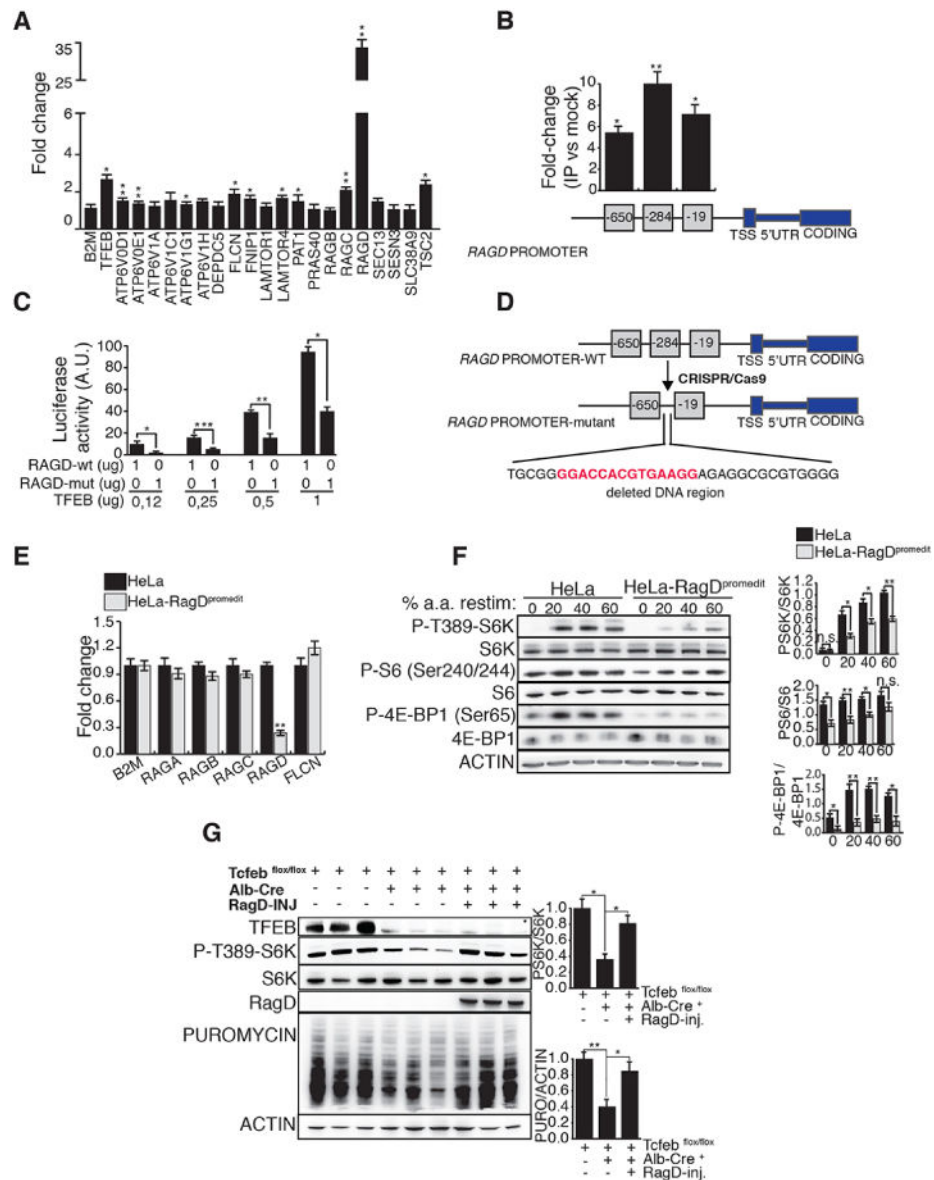


Fig 2. MiT/TFE transcription factors control mTORC1 activity through RagD

(A) mRNA levels of mTORC1-related genes in *TFEB*-CA HeLa cells treated with doxycycline. Values were normalized relative to *HPRT1* and expressed as fold change relative to untreated cells. (B) ChIP analysis of TFEB binding to *RagD* promoter in doxycycline treated HeLa *TFEB*-CA cells. Squares represent CLEAR sites in *RagD* promoter and numbers refer to their distance (bp) from the transcriptional start site (TSS). Immuno-precipitated DNA was normalized to the input and plotted as relative enrichment over a mock control. (C) Luciferase assay analysis after transfection of increasing amounts of *TFEB* construct was performed in HeLa cells co-transfected with a wild type (RAGD-wt) or mutated (RAGD-mut) *RagD*-promoter luciferase reporter plasmids. (D) Scheme of CRISPR/Cas9-mediated mutation in the endogenous *RagD* promoter of HeLa cells. A region of 33bp containing the CLEAR site at position -284 (in red) was ablated. (E) Transcript levels of *Rags* and *Flcn* genes were analyzed in the mutated HeLa cell line

(HeLa-RagD^{promedit}) versus control HeLa and normalized relative to *HPRT1* gene. (F) Immuno-blotting analysis of mTORC1 signaling in HeLa-RagD^{promedit} cells compared to control HeLa. The ratio of phosphorylated/total protein levels were shown for the indicated mTORC1 substrates. The plots in (A), (B), (C), (E), (F) represent mean \pm SEM of 3 independent experiments (Student t test). (G) Mice with indicated genotypes were nutritionally synchronized and injected with puromycin 30 minutes prior sacrifice. Where indicated Tcfef^{flox/flox}; Alb-Cre⁺ mice were injected with an AAV-vector carrying human *RagD* cDNA. Liver lysates were analyzed for phosphorylation of S6K and levels of puromycin incorporation. The plots show means of triplicates \pm SEM, Anova (one-way) expressed as ratio of phosphorylated S6K/pan-S6K and puromycin/actin. In (A), (B), (C), (E), (F), (G) *p <0.05, **p <0.01, ***p <0.001.

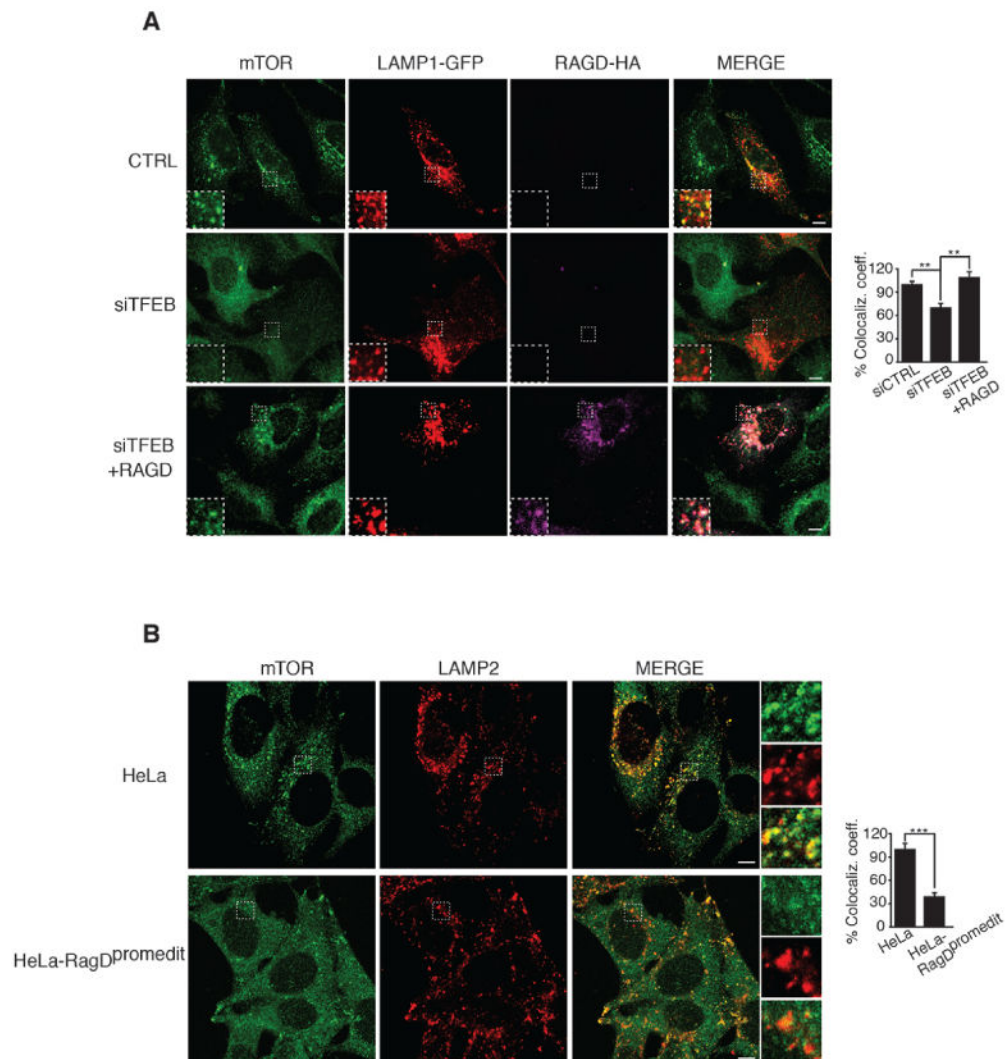


Fig 3. MiT/TFE transcription factors promote lysosomal recruitment of mTOR upon nutrient loading

(A) Representative immunofluorescence images of endogenous mTOR, LAMP1-GFP (visualized as red) and RAGD-HA in HeLa cells. Cells were transfected with scramble (*CTRL*) or with *TFEB* siRNA (siTFEB) and after 48 hours with *LAMP1-GFP* and with *RagD-HA* plasmids for additional 24 hours. (B) Representative immunofluorescence images of mTOR and LAMP2 in HeLa-RagD^{promedit} and in control HeLa cells. (A,B) Cells were deprived of a.a. for 50 minutes and then stimulated with a.a. for 15 minutes. The plots represent quantification of the data from 15 cells per condition from three independent experiments. Results are shown as means of co-localization coefficient of mTOR and LAMP1 ± SEM (Anova, one-way) in (A) of mTOR and LAMP2 ± SEM (Student t test) in (B). (**p < 0.01, ***p < 0.001). Scale bars 10 μm.

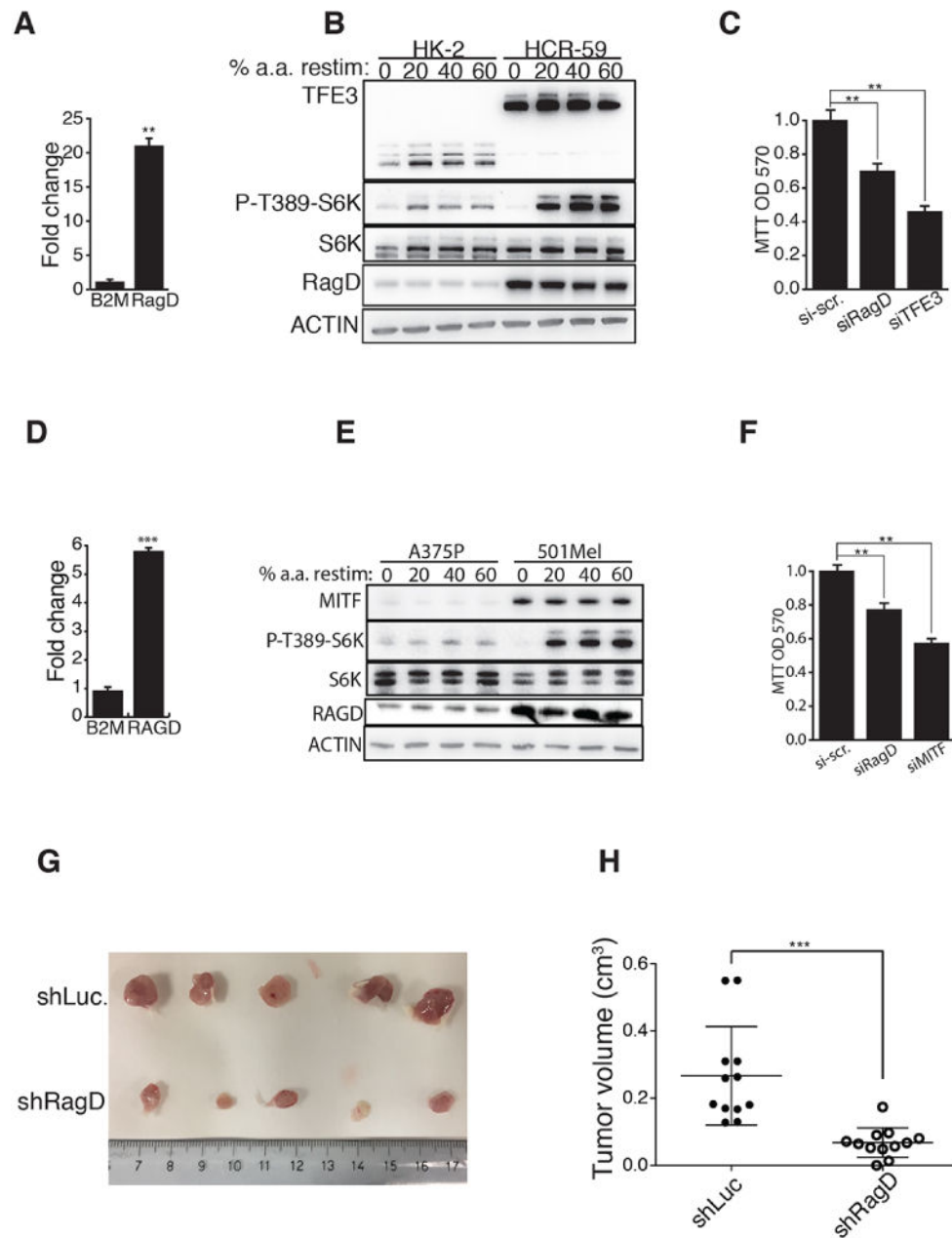


Fig 4. Deregulation of the MiT/TFE-RagD-mTORC1 regulatory axis supports cancer growth (A) mRNA levels of *RagD* in a cell line from a patient with RCC (HCR-59) relative to control kidney cells (HK-2). *B2M* expression was shown as control unrelated gene. Gene expression was normalized relative to *HPRT1*. The plot represents means of three independent experiments \pm SEM; Student t test. (B) Analysis of S6K phosphorylation at threonine 389 in HK-2 and HCR-59 cells 50 min starved for a.a. (0) and then stimulated with increasing levels of amino acids for 20 min. (C) Proliferation levels of HCR-59 cells transfected with *scramble* (*SCR*), *RagD* or *TFE3* siRNAs. The plot represents means of three independent experiments \pm SEM; Anova (one way). (D) MITF-dependent melanoma patient-derived cells (501Mel) were analyzed for mRNA levels of *RagD* (*B2M* expression

was shown as control unrelated gene). Values were expressed as relative to control melanoma cells (A375P). Gene expression was normalized relative to *HPRT1*. The plot represents means of three independent experiments \pm SEM (Student t test). (E) Representative immunoblotting analysis for the indicated proteins in control (A375P) and MITF-dependent melanoma (501Mel) cells stimulated with increased levels of amino acids. (F) Proliferation index of 501Mel cells transfected with *scramble (SCR)*, *RagD* or *MITF* siRNAs. The plot represents means of three independent experiments \pm SEM; Anova (one way). (G,H) 501Mel cells were infected with a lentivirus expressing a short harpin RNA targeting the *Luciferase* (control, Sh-Luc) or *RagD* mRNAs and transplanted in NSG mice. (G) Representative picture of tumors isolated from both groups of mice. (H) Plot shows tumor volumes. Each dot represents a tumor. 12 tumors (n=12 mice) were analyzed per group; Student t test. In (A), (C), (D), (F), (H) **p<0.01, ***p < 0.001.